Laboratory Investigation (2017) 97, 232–242
© 2017 USCAP, Inc All rights reserved 0023-6837/17

Fibroblastic foci, covered with alveolar epithelia exhibiting epithelial–mesenchymal transition, destroy alveolar septa by disrupting blood flow in idiopathic pulmonary fibrosis

Miki Yamaguchi[1], Sachie Hirai[1], Yusuke Tanaka[1,2], Toshiyuki Sumi[1,2], Masahiro Miyajima[3], Taijiro Mishina[3], Gen Yamada[2], Mitsuo Otsuka[2], Tadashi Hasegawa[4], Takashi Kojima[5], Toshiro Niki[6], Atsushi Watanabe[3], Hiroki Takahashi[2] and Yuji Sakuma[1]

Idiopathic pulmonary fibrosis (IPF) is a chronic, progressive interstitial lung disease of unknown cause. IPF has a distinct histopathological pattern of usual interstitial pneumonia in which fibroblastic foci (FF) represent the leading edge of fibrotic destruction of the lung. Currently there are three major hypotheses for how FF are generated: (1) from resident fibroblasts, (2) from bone marrow-derived progenitors of fibroblasts, and (3) from alveolar epithelial cells that have undergone epithelial–mesenchymal transition (EMT). We found that FF dissociated capillary vessels from the alveolar epithelia, the basement membranes of which are fused in normal physiological conditions, and pushed the capillaries and elastic fibers down ~100 μm below the alveolar epithelia. Furthermore, the alveolar epithelial cells covering the FF exhibited a partial EMT phenotype. In addition, normal human alveolar epithelial cells *in vitro* underwent dynamic EMT in response to transforming growth factor-β signaling within 72 h. Because it seems that resident fibroblasts or bone marrow-derived cells cannot easily infiltrate and form FF between the alveolar epithelia and capillaries in tight contact with each other, FF are more likely to be derived from the epithelial-to-mesenchymal transitioned alveolar epithelia located over them. Moreover, histology and immunohistochemistry suggested that the FF formed in the lung parenchyma disrupt blood flow to the alveolar septa, thus destroying them. Consequently, collapse of the alveolar septa is likely to be the first step toward honeycombing in the lung during late stage IPF. On the basis of these findings, inhibition of transforming growth factor-β signaling, which can suppress EMT of the alveolar epithelial cells *in vitro*, is a potential strategy for treating IPF.

Laboratory Investigation (2017) **97,** 232–242; doi:10.1038/labinvest.2016.135; published online 12 December 2016

Idiopathic pulmonary fibrosis (IPF) is a chronic, progressive, irreversible interstitial lung disease of unknown cause. Its prognosis is devastating, with >50% of patients dying within 3 years after diagnosis.[1–4] Of the clinically used drugs nintedanib and pirfenidone, both of which can slow IPF disease progression, neither results in a significant decrease in the IPF mortality rate.[5] IPF has a distinct histopathological pattern of usual interstitial pneumonia that includes a number of small areas consisting of fibroblasts, myofibroblasts, and abundant extracellular matrix, known as fibroblastic foci (FF).[1,2,6] In tissue sections, FF can be clearly visualized by alcian blue (AB) staining and usually present as sharp demarcations.[7] These foci are generally accepted as the structures predominantly responsible for the fibrotic destruction/distortion of the lung architecture in IPF.[1–4]

The source of fibroblasts as a component of FF is still under debate; however, there are three major hypotheses for how

[1]Department of Molecular Medicine, Research Institute for Frontier Medicine, Sapporo Medical University School of Medicine, Sapporo, Japan; [2]Department of Respiratory Medicine and Allergology, Sapporo Medical University School of Medicine, Sapporo, Japan; [3]Department of Thoracic Surgery, Sapporo Medical University School of Medicine, Sapporo, Japan; [4]Department of Surgical Pathology, Sapporo Medical University School of Medicine, Sapporo, Japan; [5]Department of Cell Science, Research Institute for Frontier Medicine, Sapporo Medical University School of Medicine, Sapporo, Japan and [6]Department of Pathology, Jichi Medical University School of Medicine, Tochigi, Japan

Correspondence: Dr Y Sakuma, MD, PhD, Department of Molecular Medicine, Research Institute for Frontier Medicine, Sapporo Medical University School of Medicine, South 1, West 17, Chuo-ku, Sapporo 060-8556, Japan.
E-mail: sakuma@sapmed.ac.jp

Received 10 August 2016; revised 28 October 2016; accepted 10 November 2016

Table 1 COSMIC mutations identified in the HuL cells analyzed

Age/sex	HuL	Gene name	Mutation ID	AA mutation	CDS mutation
71/M	4	SMARCB1	COSM1090		c.1119-41G>A (intron)
61/M	5	PDGFRA	COSM22413	p.V842V (silent)	c.2472C>T
		NOTCH1	COSM13047	p.V1578delV	c.4732_4734delGTG
		PTEN	COSM5915		c.1-9C>G (intron)
65/F	6	PDGFRA	COSM22413	p.V842V (silent)	c.2472C>T

Abbreviations: AA, amino acid; CDS, coding sequence; COSMIC, catalog of somatic mutations in cancer; del, deletion; F, female; M, male.

these cells are generated in the lung: (1) from resident fibroblasts, (2) from bone marrow-derived progenitors of fibroblasts (also known as fibrocytes), and (3) from alveolar epithelial cells that have undergone epithelial–mesenchymal transition (EMT).[1,3] IPF-related inflammation is usually mild and is not considered the leading cause of fibrogenesis in the IPF lung.[1–4] Instead, injured alveolar epithelial cells that secrete transforming growth factor-β (TGF-β), the major cytokine regulating EMT and fibrosis,[8,9] seem to be the key driver in IPF disease initiation. Several articles support the hypothesis that fibroblasts in FF are derived from alveolar epithelia that exhibit EMT phenotype, on the basis of histopathological and cell biological findings, or murine models of cytokine-mediated pulmonary fibrosis.[10–13] Conversely, one report did not find evidence of EMT in the pathogenesis of pulmonary fibrosis.[14] More importantly, the mechanisms by which small FF cause destruction of the preexisting lung structure remain to be determined. However, by dividing alveolar septa into 'alveolar domes' and 'lateral walls of alveoli' according to a report by Itoh *et al*,[15] we can identify the probable first mechanism by which FF distort lung architecture.

In the present study, we demonstrate that (1) alveolar epithelial cells from normal human lung tissues undergo dynamic EMT or mesenchymal-to-epithelial transition (MET); (2) histological and immunohistochemical findings of IPF lungs support alveolar epithelial EMT as the source of FF; and (3) FF disrupt blood flow to alveoli lateral walls, thus destroying them, which seems to be the first step of architectural remodeling in the IPF lung.

MATERIALS AND METHODS

All experimental procedures were approved by the Institutional Review Board at Sapporo Medical University.

Isolation and Preparation of Human Alveolar Epithelial Cells

Alveolar epithelial cells were isolated from macroscopically normal lung tissues (range: ~3–21 g in weight) obtained from three patients (2 males, 1 female: age range 61–71 years) who were operated on for lung adenocarcinoma at Sapporo Medical University Hospital (Table 1). Written, informed consent was obtained from each patient. First, we excluded mesothelial cells from the tissues as follows: briefly tissues were rinsed with phosphate buffered saline containing penicillin-streptomycin (1:100, Nacalai Tesque, Kyoto, Japan) and amphotericin B (2.5 μg/ml, Sigma-Aldrich, St Louis, MO, USA), and then incubated with Dulbecco's modified Eagle's medium (DMEM) containing collagenase/dispase (1 mg/ml, Sigma-Aldrich) at 37 °C for 15 min. Next, DMEM containing dispase II (2.0 unit/ml, Sigma-Aldrich) was instilled into the distal air spaces and the lung tissue was incubated in DMEM containing collagenase/dispase (1 mg/ml) at 37 °C for 30 min. The digested lung tissue was then minced and incubated for another 30 min, and the suspension was filtered through a 100 μm Nylon Cell Strainer (Thermo Fisher Scientific Japan, Yokohama, Japan) and centrifuged at 1500 rpm for 5 min. The cell pellet was subsequently resuspended and incubated in phosphate buffered saline containing PharmLyse (BD Biosciences, San Jose, CA, USA) at room temperature for 5 min and then centrifuged at 1500 rpm for 5 min. The cells (5.0×10^5) were seeded onto 100 mm cell culture dishes (#353003, Falcon, Corning, NY, USA) that had been pre-seeded with mitomycin-C-treated NIH3/T3 cells (2.88×10^5 cells/dish) as feeder cells. Cultures were maintained in bronchial epithelial cell growth medium (BEGM, Lonza Japan, Tokyo, Japan), a serum-free media, for 11 days. On reaching sub-confluence, cells were trypsinized and used for experimentation as described below. Cells derived from each of the three lung tissues, selected in BEGM culture, were termed human lung (HuL) 4, 5, or 6 cells and were characterized in detail in this study. Sequencing analysis using Ion AmpliSeq Cancer Hotspot Panel v2 (Thermo Fisher Scientific) revealed that HuL4–6 cells had very few mutations in the 50 oncogenes or tumor suppressor genes analyzed (Table 1), supporting that the characterized polyclonal HuL4–6 cells were derived from normal alveolar epithelial cells, not from lung adenocarcinoma cells.

HuL Cell Culture

HuL4–6 cells were seeded onto 60-mm tissue culture dishes coated with collagen type I (#4010-010, IWAKI, AGC Techno

Glass, Tokyo, Japan) and cultured in BEGM at 37 °C in a humidified incubator with 5% CO_2. Cells were treated in the absence or presence of TGF-β1 (PeproTech, Rocky Hill, NJ, USA) or the potent and selective TGF-β receptor type I inhibitor, EW-7197 (Selleck Chemicals, Houston, TX, USA),[16] alone or in combination. Nintedanib, a triple angiokinase inhibitor for VEGFR1/2/3, FGFR1/2/3, and PDGFRα/β (Selleck) was used to examine EMT suppression in HuL4–6 cells.[5]

Immunocytochemistry

Cells grown on 35-mm glass bottom, collagen-coated dishes (D11134H; Matsunami Glass, Osaka, Japan) were fixed with 4% paraformaldehyde at room temperature for 15 min followed by permeabilization with 0.5% Triton-X 100 for 2 min. After the cells were rinsed with tris-buffered saline (TBS), they were blocked with Image-iT FX Signal Enhancer (Thermo Fisher Scientific) for 30 min and then incubated in 3% BSA/TBS for another 60 min at room temperature. Samples were then incubated overnight at 4 °C with the following primary antibodies: anti-thyroid transcription factor-1 (TTF-1) (D2E8; 1:50 dilution; Cell Signaling Technology Japan, Tokyo, Japan), anti-napsin A (TMU-Ad02; 0.5 μg/ml; Immuno-Biological Laboratories, Gunma, Japan), anti-E-cadherin (24E10; 1:400; Cell Signaling), anti-Keratin 7 (D1E4; 1:400; Cell Signaling), and anti-vimentin (V9; 1:400; Biocare Medical, Concord, CA, USA). Samples were subsequently incubated with secondary antibodies Alexa Fluor 488-conjugated goat anti-rabbit IgG, Alexia Fluor 488-conjugated donkey anti-mouse IgG, Alexa Fluor 594-conjugated goat anti-rabbit IgG, or Alexia Fluor 594-conjugated donkey anti-mouse IgG (1:400, Thermo Fisher Scientific). For the staining of fibrous actin, we used Alexia Fluor 594-conjugated Phalloidin (1:400, Thermo Fisher Scientific). After mounting of cells and staining nuclei using SlowFade Diamond Antifade Mountant with DAPI (Thermo Fisher Scientific), cells were observed via fluorescent microscopy (IX-71; Olympus, Tokyo, Japan) and photographed (DP80; Olympus).

RNA Interference Assay

Cells (5.0×10^5) were plated in 60-mm tissue culture dishes coated with collagen type I (IWAKI). In parallel, cells were transfected with either negative control (NC) siRNA (1027281; Qiagen, Valencia, CA, USA), ON-TARGETplus SMARTpool siRNA targeting ZEB1 (GE Healthcare, Buckinghamshire, England) or Silencer Select siRNA targeting SNAI1 (Ambion #s13185; ThermoFisher Scientific) using Lipofectamine RNAiMAX Reagent and OPTI-MEM I (Thermo Fisher Scientific), according to the manufacturer's recommendations.

RNA Isolation and Quantitative Reverse-Transcriptase Polymerase Chain Reaction (RT-PCR)

Total RNA extraction and quantitative RT-PCR were carried out as previously described.[17,18] The following PCR primers were all purchased from Qiagen (QuantiTect Primer Assay): β-actin, encoded by the *ACTB* gene (Hs_ACTB_1_SG); E-cadherin, encoded by the *CDH1* gene (Hs_CDH1_1_SG); TTF-1, encoded by the *NKX2-1* gene (Hs_NKX2-1_1_SG); vimentin, encoded by the *VIM* gene (Hs_VIM_1_SG); N-cadherin, encoded by the *CDH2* gene (Hs_CDH2_1_SG); zinc finger E-box binding homeobox 1 (ZEB1), encoded by the *ZEB1* gene (Hs_ZEB1_2_SG); and SNAI1, encoded by the *SNAI1* gene (Hs_SNAI1_1_SG). Beta-actin was used to standardize the quantity of target mRNAs. Relative mRNA expression levels were calculated using the comparative $\Delta\Delta C_T$ method and are presented as the averages of triplicate experiments.

Western Blotting

Treated cells were lysed in NuPAGE LDS Sample Buffer (Thermo Fisher Scientific). Whole cell lysates were subjected to SDS-PAGE (4–15% Mini-Protean TGX Precast Gels; BIO-RAD, Hercules, CA, USA) followed by blotting with specific antibodies, and detection using the Supersignal West Pico Chemiluminescent Substrate (Thermo Fisher Scientific). The primary antibodies used were anti-E-cadherin (24E10; 1:1000; Cell Signaling), anti-TTF-1 (EPR8190; 1:1000; Abcam Japan, Tokyo, Japan), anti-phospho-SMAD2 (S465/467) (D27F4; 1:1000; Cell Signaling), anti-vimentin (D21H3; 1:1000; Cell Signaling), and anti-vinculin (hVIN-1; 1:5000; Sigma-Aldrich). To evaluate the relative expression levels of E-cadherin, the band intensities were measured on X-ray film using Image J software (National Institutes of Health, Bethesda, MD, USA).

IPF Tissues

IPF lung tissues obtained from four patients treated at the Sapporo Medical University Hospital were analyzed. All patients were male, with a median age of 71.5 years (range: 66–75 years), and fulfilled the current diagnostic criteria for IPF (Table 2).[19] All pathological slides were reviewed and

Table 2 Clinicopathological findings in the four IPF patients analyzed

Patient	Age/sex	Lung tissue	Pathology
1	74/M	lobectomy	UIP+SqCC
2	75/M	lobectomy	UIP+SqCC
3	69/M	VATS biopsy	UIP
4	66/M	VATS biopsy	UIP

Abbreviations: M, male; SqCC, squamous cell carcinoma; UIP, usual interstitial pneumonia; VATS, video-assisted thoracic surgery.

evaluated by one author (YS). Formalin-fixed, paraffin-embedded tissues from IPF lungs were serially sectioned into 4 μm thick slices. Three serial sections were stained with AB, elastica van Gieson (EvG), and hematoxylin-eosin (H&E), or with AB-periodic acid-Schiff (AB-PAS), EvG, and H&E for histological evaluation. The remaining sections were used for immunohistochemical detection of CD34, cytokeratin 7, TTF-1, and vimentin. Whole tissue sections were retrieved using Novocastra Epitope Retrieval Solution 1 for CD34 expression or Epitope Retrieval Solution 2 (Leica Biosystems, Nußloch, Germany) for expression of the other antigens at 100 °C for 20 min. The primary antibodies used were anti-CD34 (NU-4A1; 1:8; Nichirei Biosciences, Tokyo, Japan), anti-cytokeratin 7 (OV-TL 12/30; 1:4; Dako Japan, Tokyo, Japan), anti-TTF-1 (8G7G3/1; 1:1; Dako Japan), and anti-vimentin (V9; 1:20; Dako Japan). Immunohistochemistry (IHC) staining was conducted using a Leica BOND-MAX (Leica).

RESULTS

Alveolar Epithelial Cells Derived from Normal Lung Tissues Undergo Dynamic EMT or MET

We isolated, cultured, and analyzed normal alveolar epithelial cells, termed HuL4, HuL5, and HuL6 cells, from three different individuals (Table 1). The HuL cells cultured in BEGM, which expressed TGF-β1 and TGF-β receptor type I mRNA (data not shown), demonstrated similar dynamic morphological changes in the presence or absence of TGF-β signaling at 72 h (Figure 1a; Supplementary Figure S1a). HuL4–6 cells treated with EW-7197, a selective TGF-β receptor type I inhibitor,[16] clearly expressed TTF-1 (a transcription factor essential for the development of the lung) in the nuclei and napsin A (an aspartic proteinase that promotes maturation of pro-surfactant protein B) in the cytoplasm (Figures 1b and c; Supplementary Figure S1b).[20,21] These are two key molecules indicative of alveolar epithelial type II cell origin.[22] In EW-7197-treated HuL4–6 cells, where TGF-β signaling was suppressed as evidenced by loss of phospho-SMAD2 expression,[8] protein expression was markedly decreased for vimentin, slightly increased for E-cadherin, and acquired for TTF-1 (Figure 1b). In contrast, in HuL4–6 cells cultured in the absence of EW-7197, and particularly during TGF-β1 treatment, protein expression was markedly increased for vimentin, slightly decreased for E-cadherin, and almost completely lost for TTF-1 (Figure 1b). These dynamic changes in protein expression levels were confirmed to be mirrored for the expression levels of the respective mRNA (Figure 1d). Collectively, these findings indicated that the phenotype of HuL4–6 cells was dynamically changed from epithelial to mesenchymal, or vice versa, in the presence or absence, respectively, of TGF-β signaling at 72 h. Conclusively, HuL4–6 cells underwent EMT or MET with ease in response to environmental stimuli.

Moreover, immunofluorescence revealed that EW-7197-treated HuL4–6 cells displayed a distinct epithelial phenotype, showing membranous expression of E-cadherin, cytoplasmic expression of cytokeratin (CK) 7, and a weakly speckled expression of vimentin (Supplementary Figures S2a and S2b). Conversely, TGF-β1-treated HuL4–6 cells changed into elongated fibroblast-like cells, with cytoplasmic rather than membranous expression of E-cadherin, and diffuse expression of vimentin, while maintaining uniform expression of CK7 (Supplementary Figures S2a and S2b). Since CK7 is a representative alveolar epithelial cell marker, and is not expressed in mesenchymal cells including fibroblasts,[23,24] the findings mentioned above demonstrated that the analyzed HuL4–6 cells were not contaminated by lung resident fibroblasts or NIH3/T3 cells, and that TGF-β1-treated HuL4–6 cells did not completely lose their epithelial phenotype. In short, HuL4–6 cells cultured in the presence of TGF-β1 acquired a partial, but not complete, mesenchymal phenotype.[25]

ZEB1 Knockdown Slightly Induces an Epithelial Phenotype in HuL5 Cells

We also quantified mRNA expression levels of the *ZEB1* and *SNAI1* genes, which are major EMT-inducing transcription factors, in HuL4–6 cells and found them slightly elevated in the presence of TGF-β1 (Figure 2a).[8,9] However, the upregulation of ZEB1 or SNAI1 mRNA in TGF-β1-treated HuL cells seemed not to be prominent compared with that of vimentin or N-cadherin (encoded by the *CDH2* gene) mRNA (Figures 1d and 2a). When ZEB1 expression was suppressed by siRNA in HuL5 cells, the knockdown efficiency of which was ~72% at mRNA levels, expression of TTF-1 marginally increased and expression of vimentin slightly decreased although their morphology was virtually unchanged (Figures 2b and c). Conversely, SNAI1 knockdown (knockdown efficiency: ~67% at mRNA levels) did not induce apparent changes in TTF-1 or vimentin expression in the cells (Figure 2c). These findings raise the possibility that ZEB1, not SNAI1, plays a role in EMT induction in HuL5 cells.

Fibroblastic Foci are in Direct Contact with Alveolar Epithelia and Pushdown Capillary Vessels

AB staining enabled FF to be easily identified in the IPF lungs examined (Figure 3; Supplementary Figures S3–S5). IHC revealed that FF were covered with alveolar epithelia that were uniformly and focally positive for CK7 and TTF-1, respectively, with some alveolar epithelial cells also expressing vimentin (Figure 3; Supplementary Figures S4 and S5). In addition, most of the alveolar epithelia over FF were flat rather than round, and appeared to have acquired a partial EMT phenotype.[25] It is well-known that epithelial and capillary basement membranes in the alveolar septa are irregularly fused in physiological conditions,[22] and IHC showed that capillary vessels expressing CD34 were located immediately under the CK7-positive alveolar epithelia in the near-intact parts of the examined IPF lungs (Supplementary Figure S3a). However, we found that FF pushed the capillary

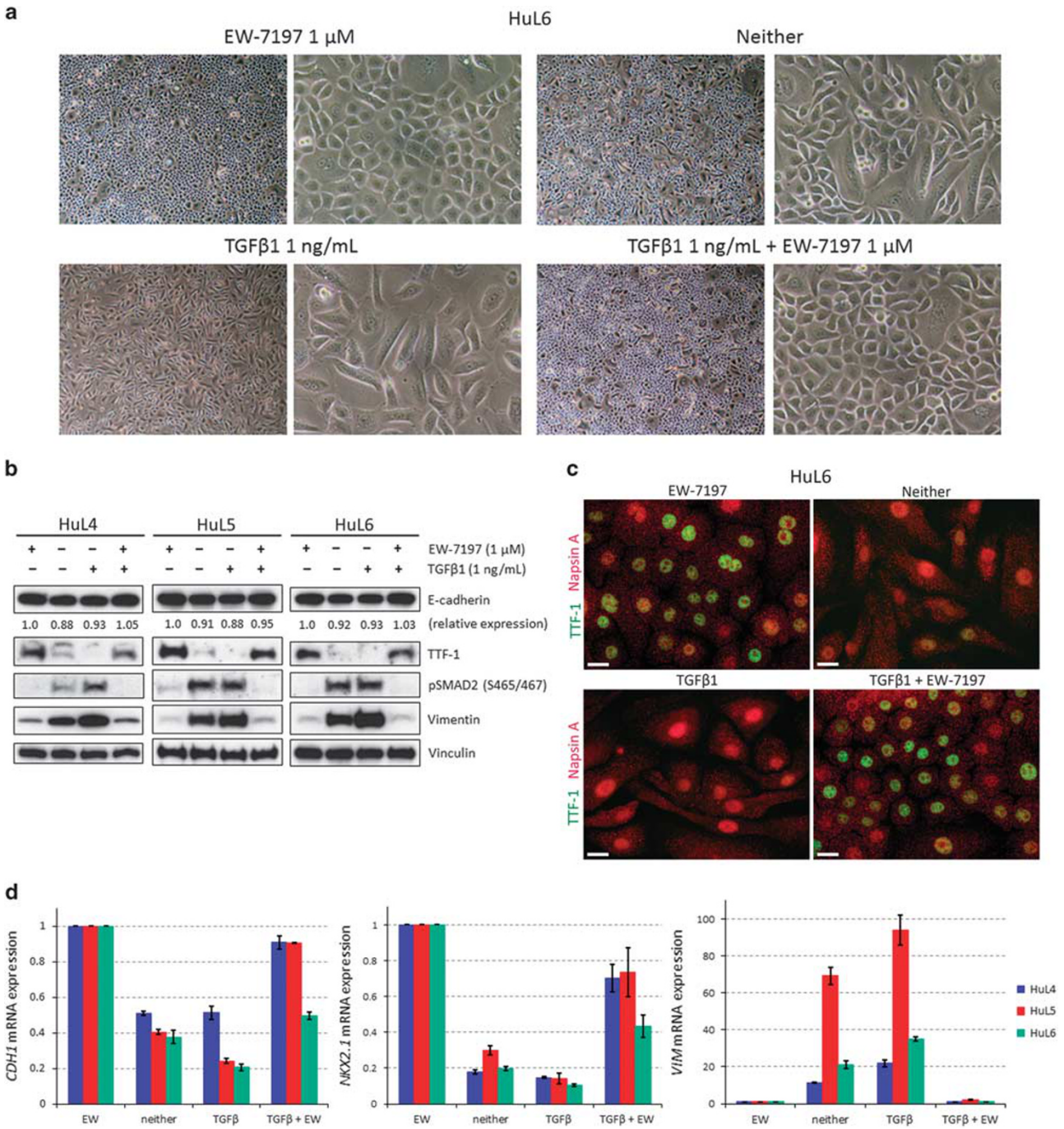

Figure 1 HuL cells undergo dynamic EMT or MET. (**a**) Representative phase-contrast images of HuL6 cells treated with EW-7197, TGF-β1, both, or neither for 72 h. (**b**) Western blots of HuL4, HuL5, and HuL6 cells treated with EW-7197, TGF-β1, both, or neither for 72 h. (**c**) Representative immunofluorescent images of HuL6 cells treated with EW-7197, TGF-β1, both, or neither for 72 h. Scale bars, 20 μm. (**d**) Quantitative RT-PCR for the expression of *CDH1*, *NKX2-1*, and *VIM* mRNA in HuL4–6 cells cultured for 72 h. The mRNAs were measured in triplicate. Results are expressed as the mean ± s.d.

vessels and elastic fibers down ~100 μm below the alveolar epithelia (Figure 3; Supplementary Figures S3–S5). This means that FF, not capillary vessels, are in contact with alveolar epithelia exhibiting a partial EMT phenotype, and the foci exclude capillary vessels and elastic fibers, the major preexisting components in the alveolar septa.[22] It appears to be hard for resident fibroblasts or bone marrow-derived fibrocytes to infiltrate and proliferate between alveolar epithelia and capillary vessels, the basement membranes of which are physiologically fused.[22] Thus, FF are more likely to

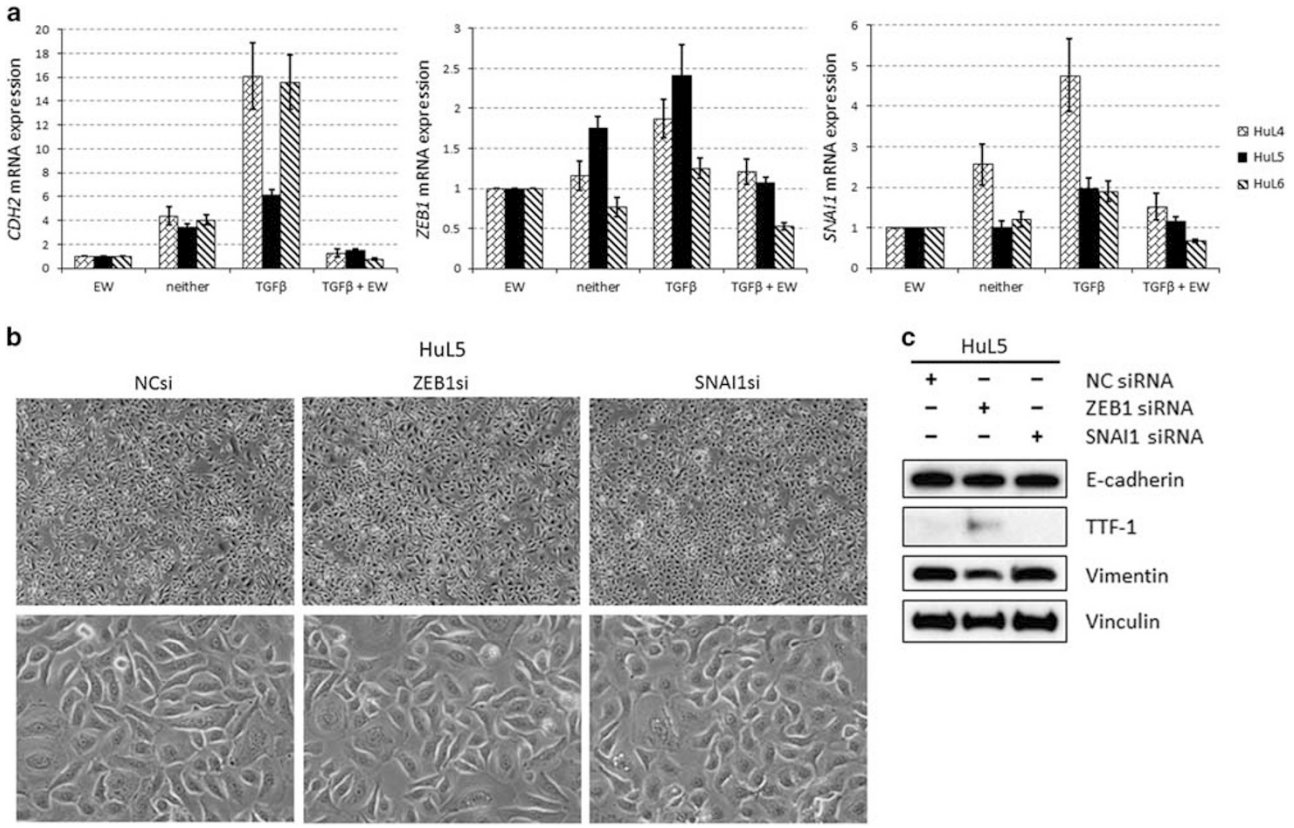

Figure 2 ZEB1 knockdown slightly inhibits EMT in HuL5 cells. (**a**) Quantitative RT-PCR for the expression of *CDH2*, *ZEB1*, and *SNAI1* mRNA in HuL4–6 cells treated with EW-7197, TGF-β1, both, or neither for 72 h. The mRNAs were measured in triplicate. Results are expressed as the mean ± s.d. (**b**) Representative phase-contrast images of HuL5 cells transfected with NC siRNA (20 nM), ZEB1-specific siRNA (20 nM), or SNAI1-specific siRNA (20 nM) that were cultured for 72 h. (**c**) Western blots examining the effects of ZEB1 or SNAI1 depletion by specific siRNA in HuL5 cells.

be derived from the transitioned alveolar epithelia located over them. IHC also demonstrated that the fibroblasts within FF lacked expression of CK7 and stained diffusely positive for vimentin, suggesting that they had completely lost their epithelial features (Figure 3; Supplementary Figures S4 and S5).

Fibroblastic Foci Disrupt Blood Flow to Alveolar Septa, Leading to Destruction of the Lung Architecture

We would like to propose a new hypothesis of how FF distort the preexisting structure of the lung. Alveolar ducts extend longitudinally and latitudinally in the lung parenchyma, and the inner surface of the duct is covered with sheets of alveoli.[15,22] In this study, we divided alveolar septa into 'alveolar domes' and 'lateral walls of alveoli,' following the definition by a previous report,[15] thereby gaining a deeper understanding of the first step toward distortion/destruction of preexisting architecture in the IPF lung (Figure 4a). Although alveolar domes have small vessels (arterioles or venules) as well as capillary vessels, alveoli lateral walls contain only capillary vessels,[15] indicating that a lateral wall completely relies on its alveolar dome for blood supply. We found that FF often formed not only in subpleural/paraseptal areas, but also in alveolar domes, and the alveolar domes affected by FF almost never had branching lateral walls of alveoli over the foci (Figure 3; Supplementary Figures S3 and S5). The disappearance of alveoli lateral walls over FF is probably a result of the foci formation, because this process dissociates the capillary vessels from the alveolar epithelia, whose basement membranes are physiologically fused.[22] Once a fibroblastic focus has formed in a portion of an alveolar dome, the focus, which lacks capillaries within it, disrupts blood flow from the alveolar dome to the lateral wall(s), leading to a subsequent collapse of the alveolar septa (Figure 3; Supplementary Figures S3 and S5). Our hypothesis that the FF within alveolar domes disrupt blood flow to lateral walls on the domes and consequently destroy them, is also supported by Figure 4b. We surmise that such collapse of the alveolar septa is the first step toward honeycombing in the lung during late stage IPF.[1,6]

Nintedanib does not Inhibit EMT in HuL Cells

We next explored if nintedanib, an approved drug for IPF treatment,[5] had an effect on EMT or MET in HuL4–6 cells. In the presence of EW-7197, all the HuL cells showed a cobblestone-like appearance, clearly expressed TTF-1, and

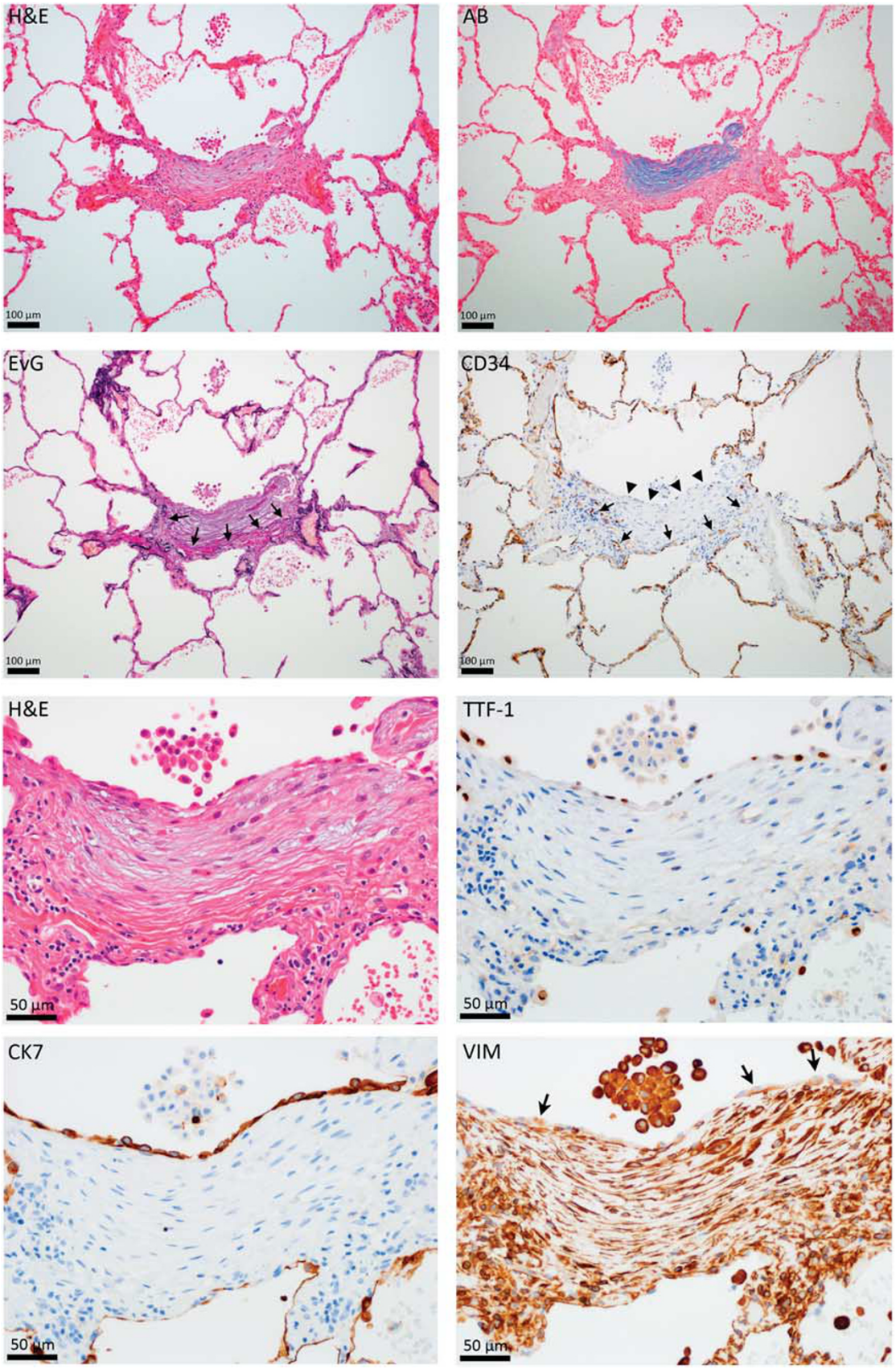
H&E
100 μm
AB
100 μm
EvG
100 μm
CD34
100 μm
H&E
50 μm
TTF-1
50 μm
CK7
50 μm
VIM
50 μm

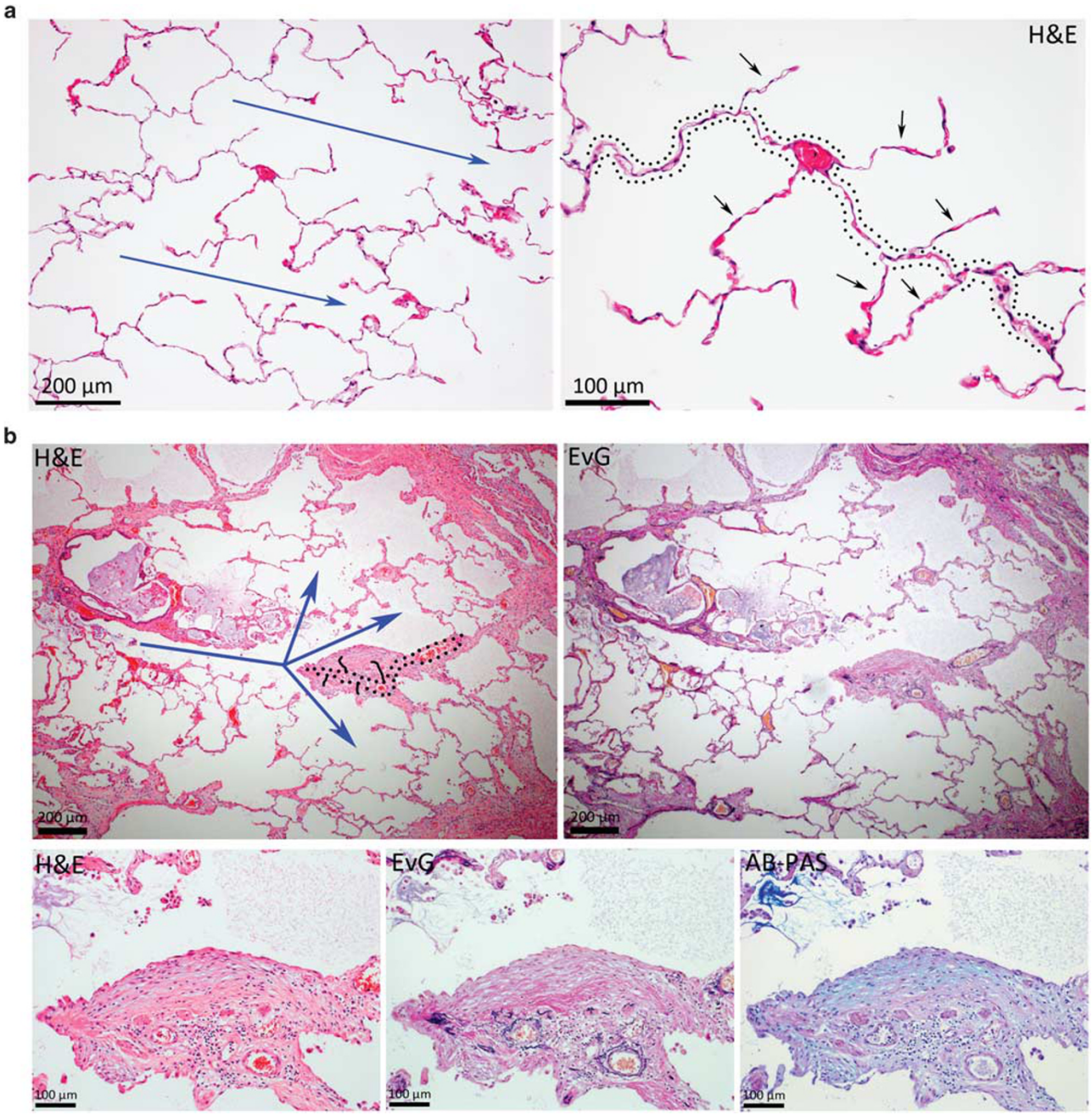

Figure 4 Alveoli lateral walls disappear in the alveolar dome affected by fibroblastic foci. (**a**) An example of near-normal lung tissue is shown (H&E staining). (Left) Blue arrows indicate the airflow of two alveolar ducts. (Right) An alveolar dome is accompanied by dotted lines and the alveoli lateral walls are indicated by black arrows. (**b**) (Upper left) Blue arrows indicate the airflow of a respiratory bronchiole and its downstream alveolar ducts. Dotted lines and solid lines indicate 'predicted' alveolar dome and its lateral walls, respectively, which presumably existed before the fibroblastic foci were formed. (Upper right and lower) Two fibroblastic foci are observed at both sides of the alveolar dome.

Figure 3 A fibroblastic focus is shown pushing capillary vessels and elastic fibers down to make a sharp demarcation. Staining with H&E, AB, and EvG, and immunohistochemistry for CD34, TTF-1, cytokeratin 7, and vimentin (VIM) expression in a fibroblastic focus observed in Patient 1. Capillaries expressing CD34 were not observed immediately under the alveolar epithelia covering the fibroblastic focus (arrowheads in CD34 panel). The focus was observed to push the elastic fibers and capillaries down, thus showing a pushing margin (arrows in EvG and CD34 panels). The alveolar epithelia over the fibroblastic focus expressed almost uniform TTF-1 and CK7 (TTF-1 and CK7 panels), with some epithelia also positive for VIM (arrows in VIM panel).

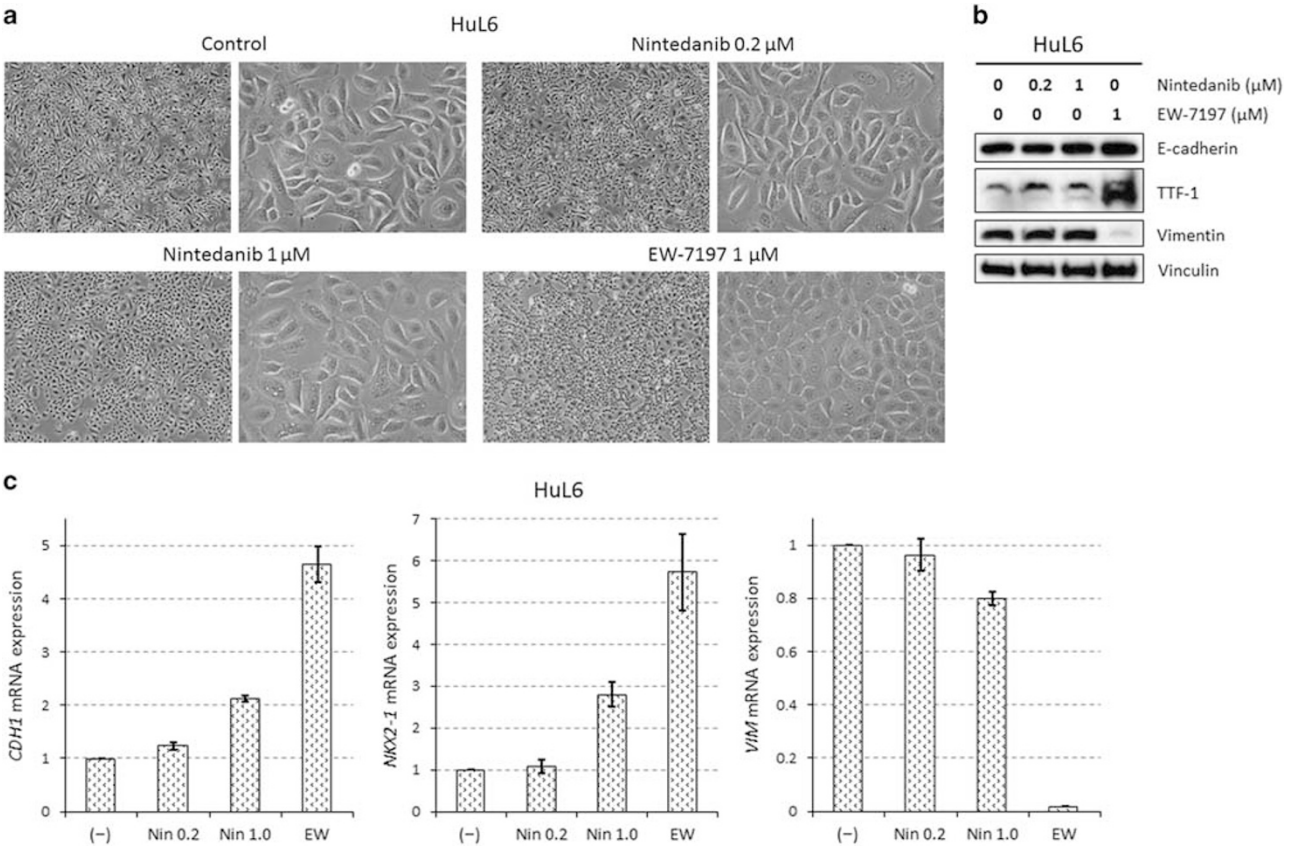

Figure 5 Unlike EW-7197, nintedanib does not inhibit EMT in HuL6 cells. (**a**) Representative phase-contrast images of HuL6 cells treated with nintedanib (0.2 or 1 μM), EW-7197 (1 μM), or neither for 72 h. (**b**) Western blots of HuL6 cells treated with nintedanib (0.2 or 1 μM), EW-7197 (1 μM), or neither for 72 h. (**c**) Quantitative RT-PCR for the expression of *CDH1*, *NKX2-1*, and *VIM* mRNA in HuL6 cells treated with nintedanib (0.2 or 1 μM), EW-7197 (1 μM), or neither for 72 h. The mRNAs were measured in triplicate. Results are shown as the mean ± s.d.

almost completely lost the expression of vimentin, as expected. In contrast, treatment with 0.2 μM (200 nM) nintedanib did not induce apparent changes in morphology or expression levels of the three molecules analyzed compared with control treatment (Figure 5; Supplementary Figure S6). Considering that the Cmax (peak plasma concentration after administration) of nintedanib in IPF patients who are administered with 150 mg of nintedanib twice daily seems to be between 50 and 100 nM,[26] this drug is not likely to exert its therapeutic effect in the clinic through inhibiting EMT, or by preserving an epithelial phenotype, in alveolar epithelial cells.

DISCUSSION

This study has demonstrated that (1) normal human alveolar epithelial cells (HuL cells) dynamically undergo EMT or MET in the presence or absence, respectively, of TGF-β signaling within 72 h; (2) histopathological and IHC analyses of IPF lungs suggest that FF are derived from the transitioned EMT alveolar epithelia located over them; (3) FF seem to disrupt blood flow to lateral walls of the alveoli and destroy them.

Identifying the source of FF, small areas of active fibrosis in the lung, is critically important for the development of an effective treatment for IPF, because management of IPF could be achieved by completely suppressing the formation of new FF. Although one report claims that EMT does not play a role in the pathogenesis of pulmonary fibrosis,[14] the bleomycin mouse model used in that study, which is widely used in IPF research, has its limitations, including being responsive to steroids and that the fibrosis in this model resolves itself with time.[3] We believe that both histopathological analysis of the lung tissues from IPF patients and cell biological examination of normal, not neoplastic, human alveolar epithelial cells are critical for determination of the initiation and progression of IPF. However, only one published study has analyzed both of these.[12] That study, conducted by Marmai *et al*,[12] found that non-neoplastic human alveolar epithelial cells *in vitro* can undergo EMT in response to TGF-β signaling in 5 days, and our experimental results using HuL cells are in agreement with these findings. Several studies indicate that integrin $\alpha v\beta 6$, which is expressed by alveolar epithelial cells, binds to an arginine–glycine–aspartic acid motif in a latent TGF-β complex and coverts it to an active form, thereby promoting pulmonary fibrosis.[11,12,27] Although we did not examine IPF lung tissues for the expression of integrin $\alpha v\beta 6$, a seminal

report has shown that the integrin expression is markedly upregulated in alveolar epithelia in fibrotic lungs compared with healthy lungs.[28] Our study has also presented three key histological findings that support our hypothesis that EMT contributes to the formation of FF: (1) the alveolar epithelia over FF displayed a partial EMT phenotype; (2) although epithelial and capillary basement membranes in alveolar septa are fused in physiological conditions,[22] the FF were localized between them, were in direct contact with the transitioned alveolar epithelia, and pushed the pre-existing capillaries and elastic fibers down ~100 μm below the epithelia; (3) FF consequently excluded capillary vessels from them, indicating that the foci are different from typical granulation tissues. Two of the three findings mentioned above, points 1 and 3, are compatible with previous reports,[10–13,29,30] but to our knowledge, the second finding has not yet been reported. Although it seems that resident fibroblasts or bone marrow-derived cells cannot easily infiltrate between alveolar epithelia and capillaries that are in tight contact with each other, transitioned EMT alveolar epithelia could lose their epithelial phenotype completely, form a fibroblastic focus, and as a result, exclude capillaries from the focus if a high-level of TGF-β activity is maintained. Furthermore, the histological and immunohistochemical analyses in this study led us to surmise that once a fibroblastic focus, much less than 1 mm in diameter, is formed in an alveolar dome, it will impede blood flow to the lateral wall(s) of the alveolus and consequently destroy it. This is probably the first step toward architectural remodeling in the IPF lung.

Collectively, the experimental findings in this study suggest that FF are derived from the transitioned alveolar epithelia located over them; however, our study has a few limitations. First, we examined IPF lung tissues obtained from only four patients. This is because we selected patients who fulfilled the criteria for having IPF according to the current diagnostic guidelines,[19] and then excluded lung tissues where honeycomb changes accounted for most areas of the tissues. Second, FF in the analyzed lung tissues were completely negative for CK7, whereas TGF-β1-treated HuL cells, which were mostly spindle-shaped and uniformly positive for vimentin, had preserved expression of CK7. HuL cells in the presence of TGF-β1 are likely to correspond to the transtioned alveolar epithelia over FF, rather than to the fibroblasts within the foci. It would therefore be interesting to determine whether long-term treatment of HuL cells with TGF-β1 transforms them into cells with a complete mesenchymal phenotype, like the fibroblasts in FF. However, FF might be derived from capillary components, namely from endothelial cells or pericytes;[1,4,14] therefore, further research is needed to determine the origin of the foci.

The experimental findings in the present study led us to propose that FF in the IPF lungs stem from the transitioned alveolar epithelia located over the foci, and that they disrupt the blood flow to the alveoli lateral walls, thus destroying them. This process is probably the first step toward the marked distortion of the lung architecture that occurs in IPF. Supposing that FF are indeed derived from transitioned EMT alveolar epithelia, repression of EMT will inhibit the formation of novel FF and consequently control the progression of IPF. We also examined if nintedanib was able to suppress EMT in HuL cells, because previous reports have suggested that it can inhibit EMT to some extent in cancer cell lines.[31,32] However, although the peak plasma concentration of nintedanib in IPF patients has been reported to be between 50 and 100 nM,[26] even treatment with 0.2 μM nintedanib had no obvious effects on the phenotypes of the analyzed HuL cells. These findings collectively suggest that nintedanib cannot suppress EMT in normal alveolar epithelial cells, and that its efficacy in clinical IPF treatment is probably due to mechanism(s) other than the inhibition of EMT in alveolar epithelia. In contrast, EW-7197 consistently induced a clear epithelial phenotype in HuL cells, suggesting that TGF-β receptor inhibitors might, at least partly, suppress active fibrosis in the IPF lung and control the progression of the disease. Since the effects of EW-7197 on HuL cells were partially mirrored by ZEB1 knockdown, but not SNAI1 knockdown, ZEB1 may contribute to EMT induction in HuL cells, at least in part. However, further studies focusing on EMT-inducing transcription factors are clearly needed to clarify which factor(s) play a decisive role in the EMT of alveolar epithelial cells.

In conclusion, the normal human alveolar epithelia HuL cells examined in this study underwent dynamic EMT or MET in the presence or absence, respectively, of TGF-β signaling. Histological and immunohistochemical analyses of lung tissues affected by IPF suggested that FF are more likely to be derived from the transitioned EMT alveolar epithelia covering the foci than from resident fibroblasts or bone marrow-derived cells. We also proposed the hypothesis that the presence of FF disrupts blood flow to alveolar septa and destroys them, which seems to be the first step toward advanced remodeling in the IPF lung. Although it remains to be resolved what mechanism(s) in combination with TGF-β signaling induce HuL cells into a complete EMT phenotype, TGF-β receptor inhibitors, which can suppress EMT in HuL cells, could be a valuable new approach for the treatment of IPF.

Supplementary Information accompanies the paper on the Laboratory Investigation website (http://www.laboratoryinvestigation.org)

ACKNOWLEDGMENTS

This work was supported in part by a Grants-in-Aid for Scientific Research (KAKENHI) from Japan Society for the Promotion of Science (JSPS), Grant Number 15K08364 (given to YS).

DISCLOSURE/CONFLICT OF INTEREST

The authors declare no conflict of interest.

1. King Jr TE , Pardo A, Selman M. Idiopathic pulmonary fibrosis. Lancet 2011;378:1949–1961.
2. Borensztajn K, Crestani B, Kolb M. Idiopathic pulmonary fibrosis: from epithelial injury to biomarkers-insights from the bench side. Respiration 2013;86:441–452.
3. Camelo A, Dunmore R, Sleeman MA, *et al.* The epithelium in idiopathic pulmonary fibrosis: breaking the barrier. Front Pharmacol 2014;4:173.
4. Bagnato G, Harari S. Cellular interactions in the pathogenesis of interstitial lung diseases. Eur Respir Rev 2015;24:102–114.
5. Canestaro WJ, Forrester SH, Raghu G, *et al.* Drug treatment of idiopathic pulmonary fibrosis: Systematic review and network meta-analysis. Chest 2016;149:756–766.
6. Katzenstein AL, Mukhopadhyay S, Myers JL. Diagnosis of usual interstitial pneumonia and distinction from other fibrosing interstitial lung diseases. Hum Pathol 2008;39:1275–1294.
7. Yamashita M, Yamauchi K, Chiba R, *et al.* The definition of fibrogenic processes in fibroblastic foci of idiopathic pulmonary fibrosis based on morphometric quantification of extracellular matrices. Hum Pathol 2009;40:1278–1287.
8. Ikushima H, Miyazono K. TGFbeta signalling: a complex web in cancer progression. Nat Rev Cancer 2010;10:415–424.
9. Nieto MA, Huang RY, Jackson RA, *et al.* EMT: 2016. Cell 2016;166:21–45.
10. Willis BC, Liebler JM, Luby-Phelps K, *et al.* Induction of epithelial-mesenchymal transition in alveolar epithelial cells by transforming growth factor-beta1: potential role in idiopathic pulmonary fibrosis. Am J Pathol 2005;166:1321–1332.
11. Kim KK, Kugler MC, Wolters PJ, *et al.* Alveolar epithelial cell mesenchymal transition develops in vivo during pulmonary fibrosis and is regulated by the extracellular matrix. Proc Natl Acad Sci USA 2006;103:13180–13185.
12. Marmai C, Sutherland RE, Kim KK, *et al.* Alveolar epithelial cells express mesenchymal proteins in patients with idiopathic pulmonary fibrosis. Am J Physiol Lung Cell Mol Physiol 2011;301:L71–L78.
13. Jonsdottir HR, Arason AJ, Palsson R, *et al.* Basal cells of the human airways acquire mesenchymal traits in idiopathic pulmonary fibrosis and in culture. Lab Invest 2015;95:1418–1428.
14. Rock JR, Barkauskas CE, Cronce MJ, *et al.* Multiple stromal populations contribute to pulmonary fibrosis without evidence for epithelial to mesenchymal transition. Proc Natl Acad Sci USA 2011;108:E1475–E1483.
15. Itoh H, Nishino M, Hatabu H. Architecture of the lung: morphology and function. J Thorac Imaging 2004;19:221–227.
16. Son JY, Park SY, Kim SJ, *et al.* EW-7197, a novel ALK-5 kinase inhibitor, potently inhibits breast to lung metastasis. Mol Cancer Ther 2014;13:1704–1716.
17. Sakuma Y, Matsukuma S, Nakamura Y, *et al.* Enhanced autophagy is required for survival in EGFR-independent *EGFR*-mutant lung adenocarcinoma cells. Lab Invest 2013;93:1137–1146.
18. Sakuma Y, Nishikiori H, Hirai S, *et al.* Prolyl isomerase Pin1 promotes survival in *EGFR*-mutant lung adenocarcinoma cells with an epithelial-mesenchymal transition phenotype. Lab Invest 2016;96:391–398.
19. Raghu G, Collard HR, Egan JJ, *et al.* An official ATS/ERS/JRS/ALAT statement: idiopathic pulmonary fibrosis: evidence-based guidelines for diagnosis and management. Am J Respir Crit Care Med 2011;183:788–824.
20. Yamaguchi T, Hosono Y, Yanagisawa K, *et al.* NKX2-1/TTF-1: an enigmatic oncogene that functions as a double-edged sword for cancer cell survival and progression. Cancer Cell 2013;23:718–723.
21. Brasch F, Ochs M, Kahne T, *et al.* Involvement of napsin A in the C- and N-terminal processing of surfactant protein B in type-II pneumocytes of the human lung. J Biol Chem 2003;278:49006–49014.
22. Leslie KO, Yousem SA, Colby TV. Lungs In Histology for Pathologists, 4th edn. Mills SE (eds). Lippincott Williams & Wilkins: Philadelphia, 2012; 505–539.
23. Broers JL, de Leij L, Rot MK, *et al.* Expression of intermediate filament proteins in fetal and adult human lung tissues. Differentiation 1989;40:119–128.
24. Karantza V. Keratins in health and cancer: more than mere epithelial cell markers. Oncogene 2011;30:127–138.
25. Tam WL, Weinberg RA. The epigenetics of epithelial-mesenchymal plasticity in cancer. Nat Med 2013;19:1438–1449.
26. Mross K, Stefanic M, Gmehling D, *et al.* Phase I study of the angiogenesis inhibitor BIBF 1120 in patients with advanced solid tumors. Clin Cancer Res 2010;16:311–319.
27. Sheppard D. Epithelial-mesenchymal interactions in fibrosis and repair. Transforming growth factor-β activation by epithelial cells and fibroblasts. Ann Am Thorac Soc 2015;12 Suppl 1:S21–S23.
28. Horan GS, Wood S, Ona V, *et al.* Partial inhibition of integrin alpha(v) beta6 prevents pulmonary fibrosis without exacerbating inflammation. Am J Respir Crit Care Med 2008;177:56–65.
29. Ebina M, Shimizukawa M, Shibata N, *et al.* Heterogeneous increase in CD34-positive alveolar capillaries in idiopathic pulmonary fibrosis. Am J Respir Crit Care Med 2004;169:1203–1208.
30. Cosgrove GP, Brown KK, Schiemann WP, *et al.* Pigment epithelium-derived factor in idiopathic pulmonary fibrosis: a role in aberrant angiogenesis. Am J Respir Crit Care Med 2004;170:242–251.
31. Kutluk Cenik B, Ostapoff KT, Gerber DE, *et al.* BIBF 1120 (nintedanib), a triple angiokinase inhibitor, induces hypoxia but not EMT and blocks progression of preclinical models of lung and pancreatic cancer. Mol Cancer Ther 2013;12:992–1001.
32. Huang RY, Kuay KT, Tan TZ, *et al.* Functional relevance of a six mesenchymal gene signature in epithelial-mesenchymal transition (EMT) reversal by the triple angiokinase inhibitor, nintedanib (BIBF1120). Oncotarget 2015;6:22098–22113.